A Systematic Continuous Adjoint Approach to Viscous Aerodynamic Design on Unstructured Grids

Carlos Castro[*†]
Universidad Politécnica de Madrid, Madrid, 28040, Spain

Carlos Lozano[‡] and Francisco Palacios[§]
Instituto Nacional de Técnica Aeroespacial, Torrejón de Ardoz, Madrid, 28850, Spain

and

Enrique Zuazua[**]
Universidad Autónoma de Madrid, Madrid, 28049, Spain

A continuous adjoint approach to aerodynamic design for viscous compressible flow on unstructured grids is developed. Sensitivity gradients are computed using tools of shape deformation of boundary integrals. The resulting expressions involve second order derivatives of the flow variables that require numerical solvers with greater than second order accuracy. A systematic way of reducing the order of these terms is presented. Also, the class of admissible optimization functionals is clarified. The accuracy of the sensitivity derivatives is assessed by comparison with finite-difference computations, and the validity of the overall methodology is illustrated with several design examples.

I. Introduction

The use of CFD tools in aerodynamic design optimization has grown in importance within the last decade. In gradient-based optimization techniques, the goal is to minimize a suitable cost or objective function (drag coefficient, deviation from a prescribed surface pressure distribution, etc.) with respect to a set of design variables (defining, for example, an airfoil profile or aircraft surface). Minimization is achieved by means of an iterative process which requires the computation of the gradients or sensitivity derivatives of the cost function with respect to the design variables.

Gradients can be computed in a variety of ways, the most actively pursued recently being adjoint methods[1-5], which allow the solution of general sensitivity analysis problems governed by fluid dynamics models ranging from the full potential equation to the full compressible Reynolds-averaged Navier-Stokes equations. Adjoint methods are conventionally divided into continuous and discrete. In the continuous approach, the adjoint equations are derived from the governing PDEs and then subsequently discretized, whereas in the discrete approach the adjoint equations are directly derived from the discrete governing equations.

While, the discrete adjoint method should give gradients which are closer in value to exact finite-difference gradients, the continuous adjoint method has the advantage that the adjoint system has a unique form independent of the scheme used to solve the flow-field system. Numerical studies have shown that in typical shape optimization problems in transonic flow the differences are small enough that they have no significant effect on the final result[6].

The present work focuses on the continuous adjoint approach on unstructured grids, for which several limitations have been uncovered in the past which include the apparent inability of the method to handle arbitrary cost functions

---

[*] Authors listed in alphabetical order.
[†] Assistant Professor, Departamento de Matemáticas e Informática, ETSI Caminos, Canales y Puertos.
[‡] Research Scientist, Área de Dinámica de Fluidos, Departamento de Aerodinámica y Propulsión.
[§] Research Scientist, Área de Dinámica de Fluidos, Departamento de Aerodinámica y Propulsión.
[**] Professor, Departamento de Matemáticas, Facultad de Ciencias.

and the need of flow solvers with greater than second order accuracy. The first problem is inherent to the continuous approach (either inviscid or viscous, on structured as well as unstructured grids)[7-10], but has not been encountered so far in the discrete adjoint approach. As for the second problem, it has been reported in the continuous approach for viscous flows on unstructured grids. On structured grids, where mapping to a fixed computational space is possible, this problem can be avoided[9]. The mapping technique has been extended to optimization on unstructured grids for inviscid flows[11, 12], but a generalization to viscous flows is still lacking.

The present work aims precisely at filling those gaps by presenting a systematic continuous adjoint formulation for design optimization for viscous flows which is suitable for unstructured as well as structured grids. The point of view adopted here is similar to that in[7], and solves some of the drawbacks presented there. Indeed, the need for accurate second order derivatives of the flow variables required for computing sensitivity derivatives for viscous flows is solved with the development of a systematic way of reducing the order of the higher derivative terms. Also, the class of admissible optimization functionals is clarified. In particular, it is shown that for viscous flows arbitrary functions of the pressure alone can be naturally optimized.

The organization of the paper is as follows. The exposition begins with a brief introduction to the continuous adjoint approach and a detailed review of its application to aerodynamic design using the Euler and Navier-Stokes equations. The caveats of the approach are discussed and a proposal of resolution is put forward. Next, the practical implementation of the method is described and supporting numerical results are presented. Finally, an appendix contains a compilation of useful formulae.

II. The adjoint approach to aerodynamic design optimization

A. Formulation of the problem

In what follows we will be interested in design optimization problems within the continuous adjoint approach. In aeronautic applications, the basic setup comprises a fluid domain Ω bounded by a typically disconnected boundary $\partial\Omega$ which is conventionally divided into a "far field" component Γ_∞ and a wall boundary S. Aeronautic optimization problems seek the minimization of a certain cost function, such as the deviation of the pressure on S from a prescribed pressure distribution in inverse design problems, or integrated force coefficients (drag or lift) in force optimization problems. In these examples the cost function can be defined as an integral over the wall boundary S of a suitable function f of the flow variables (collectively referred to as U).

$$J = \int_S f(U)\, ds \tag{1}$$

where ds denotes the appropriate integration measure. Cost functions involving domain integrals are also possible, but those will not be considered in the present work.

Upon deformation of the control surface S, the cost function varies due to the variation of the geometry and the change in the solution induced by the deformation. Accordingly, the variation of the cost function (1) comprises essentially two terms

$$\delta J = \int_{\delta S} f(U)\, ds + \int_S \frac{\partial f}{\partial U}\delta U ds \tag{2}$$

The first geometric term can be expanded as follows[13]

$$\int_{\delta S} f(U)\, ds = \int_S \frac{\partial f}{\partial U}\left(\delta\vec{x}\cdot\vec{\nabla}U\right) ds + \int_S f\,\delta ds \tag{3}$$

where $\delta\vec{x}$ stands for the deformation of the points defining the boundary S and δds denotes the appropriate change in the measure. If f contains geometric quantities such as the unit normal to the boundary $\vec{n}$ –as is the case, for example, in force optimization problems– Eq. (3) takes the form

$$\int_{\delta S} f\left(U,\vec{n}\right)ds = \int_{S}\frac{\partial f}{\partial U}\left(\delta\vec{x}\cdot\vec{\nabla}U\right)ds + \int_{S}\frac{\partial f}{\partial\vec{n}}\cdot\delta\vec{n}ds + \int_{S} f\,\delta ds \tag{4}$$

where $\delta\vec{n}$ is the variation in the boundary normal induced by the deformation of the boundary. The contribution of Eq. (4) is readily computable once the boundary deformation as well as the solution to the flow equations in the unperturbed geometry is known.

As for the second term of Eq. (2) that involves the variation δU of the flow variables under the perturbation. These can be obtained a priori from the solution of the linearized flow equations (subject to the appropriate boundary conditions), but this requires a flow evaluation per independent perturbation. If the design space is large, the computational cost is prohibitive. A convenient shortcut can be found by resorting to the adjoint equations, which can be understood, in a variational context, as consistency conditions for the Lagrange multipliers (the adjoint variables) which enforce the flow equations[2, 3].

B. Aerodynamic design with the Euler equations

For the sake of completeness, the case of steady inviscid, two-dimensional compressible flow will be addressed first. Although the results that will be presented are not new, the discussion will serve as an introduction to the method and to illustrate how the same systematic approach can accommodate inviscid as well as viscous optimization problems within a fully systematic and unified viewpoint.

The governing equations in this case are

$$\vec{\nabla}\cdot\vec{F} = \frac{\partial F_x}{\partial x} + \frac{\partial F_y}{\partial y} = 0 \quad \text{in } \Omega$$
$$U = \begin{pmatrix}\rho\\ \rho u\\ \rho v\\ \rho E\end{pmatrix}, \quad F_x = \begin{pmatrix}\rho u\\ \rho u^2 + P\\ \rho uv\\ \rho uH\end{pmatrix}, \quad F_y = \begin{pmatrix}\rho v\\ \rho uv\\ \rho v^2 + P\\ \rho vH\end{pmatrix} \tag{5}$$

In these definitions, ρ is the density, u, v are the Cartesian velocity components, E is the total energy and P and H are the pressure and enthalpy, given by the following relations

$$P = (\gamma - 1)\rho\left[E - \frac{1}{2}(u^2 + v^2)\right], \quad H = E + \frac{P}{\rho} \tag{6}$$

where γ is the ratio of specific heats. Eqs. (5) are subject to characteristic-type boundary conditions[14] on the far field boundary Γ_∞, and to non-transpiration boundary conditions on solid wall boundaries

$$\vec{v}\cdot\vec{n} = un_x + vn_y = 0 \quad \text{on } S$$
$$\vec{v} = (u, v), \quad \vec{n} = \left(n_x, n_y\right) \tag{7}$$

The next step in the adjoint approach amounts to defining a suitable cost function. Conventional cost functions include specified pressure distributions (inverse design), force (drag or lift) or moment coefficients, efficiency (*i.e.* lift over drag), etc. For inverse design the appropriate definitions are

$$J = \frac{1}{2}\int_{S}\left(\Delta C_p\right)^2 ds$$
$$\Delta C_p = C_p - C_p^{(d)}, \quad C_p = \frac{P - P_\infty}{C_\infty}, \quad C_\infty = \frac{1}{2}\gamma M_\infty^2 P_\infty \tag{8}$$

where $C_p^{(d)}$ is the target pressure coefficient distribution, and M_∞, P_∞ are the free-stream Mach number and pressure, respectively, whereas for force optimization

$$\begin{aligned} J &= \int_S C_p \left(n_x \cos\alpha + n_y \sin\alpha \right) ds = C_D, \quad \text{(drag coefficient)} \\ J &= \int_S C_p \left(-n_x \sin\alpha + n_y \cos\alpha \right) ds = C_L, \quad \text{(lift coefficient)} \end{aligned} \tag{9}$$

or, in compact notation,

$$J = \int_S C_p \left(\vec{n} \cdot \vec{d} \right) ds, \quad \vec{d} = \begin{cases} (\cos\alpha, \sin\alpha) & \text{(drag)} \\ (-\sin\alpha, \cos\alpha) & \text{(lift)} \end{cases} \tag{10}$$

where α is the angle of attack. S is a closed curve corresponding to the airfoil profile (or a disjoint union of several curves in the case of high-lift devices) which can be described by the parametrization $\vec{x}(\eta) = (x(\eta), y(\eta))$ with parameter η. Dot notation will be used to indicate differentiation with respect to η. If $\vec{t} = (t_x, t_y)$ denotes the unit tangent vector to the curve, the following holds

$$\begin{aligned} &\text{Unit tangent vector:} && \vec{t} = \frac{\dot{\vec{x}}}{\left|\dot{\vec{x}}\right|}, \quad \left|\dot{\vec{x}}\right| = \left|\frac{d\vec{x}}{d\eta}\right| = \sqrt{\dot{x}^2 + \dot{y}^2} \\ &\text{Unit normal vector:} && \vec{n} = \frac{(-\dot{y}, \dot{x})}{\left|\dot{\vec{x}}\right|} \\ &\text{Integration measure:} && ds = \left|\dot{\vec{x}}\right| \, d\eta \\ &\text{Curvature:} && \kappa = \frac{\dot{x}\ddot{y} - \ddot{x}\dot{y}}{\left|\dot{\vec{x}}\right|^3} = \frac{\vec{n} \cdot \ddot{\vec{x}}}{\left|\dot{\vec{x}}\right|^2} \\ &\text{Tangent derivatives:} && \partial_{tg} f(\eta) = \vec{t} \cdot \vec{\nabla} f = \frac{df}{ds} = \frac{1}{\left|\dot{\vec{x}}\right|} \frac{df}{d\eta} = \frac{1}{\left|\dot{\vec{x}}\right|} \dot{f} \\ &\text{Differential relations:} && \partial_{tg} \vec{t} = \frac{1}{\left|\dot{\vec{x}}\right|} \dot{\vec{t}} = \kappa \vec{n}, \quad \partial_{tg} \vec{n} = \frac{1}{\left|\dot{\vec{x}}\right|} \dot{\vec{n}} = -\kappa \vec{t} \end{aligned} \tag{11}$$

where a parametrization is picked for which $\vec{n}$ is the exterior unit normal. A generic deformation of the boundary can be described as follows

$$\delta\vec{x}(\eta) = \alpha(\eta)\vec{n} + \beta(\eta)\vec{t} \tag{12}$$

where tangential and normal deformations have been explicitly separated, being quantified by $\beta(\eta)$ and $\alpha(\eta)$ –not to be confused with the angle of attack–, respectively[††].

[††] Even though it is a standard fact that every sufficiently small deformation of a curve can be described by a normal deformation alone (tangent deformations being equivalent to reparametrizations of the curve), the use of non-normal deformations is nevertheless so widespread in the aeronautics literature that we prefer to keep the tangent component explicitly.

For sufficiently small values of the deformation, the following holds

$$\begin{aligned}
&\delta\dot{\vec{x}} = (\dot{\alpha} + \beta\left|\dot{\vec{x}}\right|\kappa)\vec{n} + (\dot{\beta} - \alpha\left|\dot{\vec{x}}\right|\kappa)\vec{t} \\
&\delta ds = \left(\frac{\dot{\vec{x}}\cdot\delta\dot{\vec{x}}}{\dot{x}^2+\dot{y}^2}\right)ds = \left(\partial_{tg}\beta - \alpha\kappa\right)ds \\
&\delta\vec{t} = \left(\beta\kappa + \partial_{tg}\alpha\right)\vec{n}, \quad \delta\vec{n} = -\left(\beta\kappa + \partial_{tg}\alpha\right)\vec{t}
\end{aligned} \tag{13}$$

By using Eqs. (2)–(4) and (11)–(13), the variation of the said cost functions (8) and (10) are

$$\delta\left(\frac{1}{2}\int_S \left(\Delta C_p\right)^2 ds\right) = \int_S \left(\frac{\Delta C_p}{C_\infty}(\delta\vec{x}\cdot\vec{\nabla}P) + \mathrm{K}\frac{\left(\Delta C_p\right)^2}{2}\right)ds + \frac{1}{C_\infty}\int_S \left(\Delta C_p \delta P\right)ds \tag{14}$$

where $\mathrm{K} = (\dot{\vec{x}}\cdot\delta\dot{\vec{x}})/(\dot{x}^2+\dot{y}^2)$ for inverse design, and

$$\delta\int_S C_p\left(\vec{n}\cdot\vec{d}\right)ds = \int_S \left(\frac{1}{C_\infty}(\vec{n}\cdot\vec{d})(\delta\vec{x}\cdot\vec{\nabla}P) + \mathrm{K}C_p(\vec{d}\cdot\vec{n}) + C_p(\vec{d}\cdot\delta\vec{n})\right)ds + \frac{1}{C_\infty}\int_S \left((\vec{n}\cdot\vec{d})\delta P\right)ds \tag{15}$$

for force optimization. The terms in Eqs. (14) and (15) which involve the pressure variation δP cannot be computed without explicitly solving the linearized flow equations. The alternate strategy, which has now become standard lore, is to resort to the adjoint equations, which give an elegant and computationally economical way to computing the unknown terms. The starting point is the linearized flow equations, which in the inviscid 2D case are

$$\begin{aligned}
&\vec{\nabla}\cdot\delta\vec{F} = \partial_x\left((A_x)^T M^{-1}\delta U\right) + \partial_y\left((A_y)^T M^{-1}\delta U\right) = \vec{\nabla}\cdot\left(\vec{A}^T M^{-1}\delta U\right) = 0 \quad \text{in } \Omega \\
&\vec{A}^T = \left((A_x)^T, (A_y)^T\right), \quad (A_x)^T = \frac{\partial F_x}{\partial V}, \quad (A_y)^T = \frac{\partial F_y}{\partial V}, \quad M^{-1} = \frac{\partial V}{\partial U}, \quad V = \begin{pmatrix}\rho\\ u\\ v\\ P\end{pmatrix}
\end{aligned} \tag{16}$$

where, for later convenience, the inviscid Jacobians have been written in terms of primitive variables V (see the appendix for details). Boundary conditions for δU at the wall are obtained from the linearization of the non-transpiration boundary condition (7) on the wall

$$\vec{n}\cdot\delta\vec{v} = -\left[\left(\delta\vec{x}\cdot\vec{\nabla}\right)\vec{v}\right]\cdot\vec{n} - \delta\vec{n}\cdot\vec{v} \quad \text{on } S. \tag{17}$$

On the far field boundary, the appropriate boundary conditions are obtained from those of U as follows. Let L^{-1} be the matrix of left eigenvectors of the Jacobian $\vec{n}\cdot\vec{A}^T M^{-1}$ and Λ the diagonal matrix of eigenvalues. Therefore,

$$\vec{n}\cdot\vec{A}^T M^{-1} = L\Lambda L^{-1}, \quad W = L^{-1}U \tag{18}$$

where W are characteristic variables. On the far field boundary with characteristic-type boundary conditions on the flow variables, the propagation of information is based on the sign of the eigenvalues. Along incoming characteristics –that is, for negative eigenvalues–, the corresponding characteristic variables are given in terms of

free-stream quantities such as the Mach number, the angle of attack, etc. If those are kept fixed by the perturbation, the corresponding variations vanish

$$L^{-1}\delta U\Big|_{\text{Neg. eigenvalues}} = 0. \tag{19}$$

The linearized flow equations are next multiplied by the vector of adjoint variables

$$\Psi^T = \begin{pmatrix} \psi_1 \\ \psi_2 \\ \psi_3 \\ \psi_4 \end{pmatrix}, \tag{20}$$

and integrated over the flow domain Ω

$$0 = \int_\Omega \Psi(\vec{\nabla}\cdot\delta\vec{F})d\Omega = \int_\Omega \Psi\left(\partial_x\left((A_x)^T M^{-1}\delta U\right) + \partial_y\left((A_y)^T M^{-1}\delta U\right)\right)d\Omega. \tag{21}$$

Integrating by parts in Eq. (21) gives

$$0 = -\int_\Omega \delta U^T (M^{-1})^T (\vec{A}\cdot\vec{\nabla}\Psi^T)d\Omega + \int_{\Gamma_\infty} \Psi(\vec{n}\cdot\vec{A}^T M^{-1})\delta U ds + \int_S \Psi(\vec{n}\cdot\vec{A}^T M^{-1})\delta U ds. \tag{22}$$

Each of the three terms in Eq. (22) is forced to vanish independently. The first one, which is a domain integration, vanishes provided that Ψ satisfies the steady state inviscid adjoint equation

$$(M^{-1})^T \vec{A}\cdot\vec{\nabla}\Psi^T = 0. \tag{23}$$

On the far field boundary, incoming characteristics for Ψ correspond to outgoing characteristics for δU, and viceversa. Consequently, in view of Eq. (19) it is possible to choose boundary conditions for Ψ such that

$$\Psi(\vec{n}\cdot\vec{A}^T M^{-1})\delta U = \left(\Psi L\right)\Lambda\left(L^{-1}\delta U\right) = 0 \tag{24}$$

i.e., by setting to zero the adjoint variables corresponding to outgoing characteristics[2, 7] –or positive Λ eigenvalues.

$$\Psi L\Big|_{\text{Pos. eigenvalues}} = 0 \tag{25}$$

Along incoming characteristics, the corresponding adjoint variables on the boundary are extrapolated from the interior of the domain.

All that is left from Eq. (22) is a boundary contribution at the solid wall S, which boils down to the following relation

$$0 = \int_S \Psi(\vec{n}\cdot\vec{A}^T M^{-1})\delta U ds = \int_S (\vec{n}\cdot\delta\vec{v})\left(\rho\psi_1 + \rho\vec{v}\cdot\vec{\varphi} + \rho H\psi_4\right)ds + \int_S (\vec{n}\cdot\vec{\varphi})\delta P ds \tag{26}$$

where, for convenience, the vector $\vec{\varphi} = (\psi_2, \psi_3)$ has been defined, or, equivalently,

$$\int_S (\vec{n}\cdot\vec{\varphi})\delta P ds = -\int_S (\vec{n}\cdot\delta\vec{v})\left(\rho\psi_1 + \rho\vec{v}\cdot\vec{\varphi} + \rho H\psi_4\right)ds \tag{27}$$

In view of Eqs. (14) and (15) it can be seen that if the adjoint variables satisfy the following boundary conditions

$$\begin{aligned} \vec{n}\cdot\vec{\varphi}\big|_S &= \frac{\Delta C_P}{C_\infty}, \quad \text{(inverse design)} \\ \vec{n}\cdot\vec{\varphi}\big|_S &= \frac{1}{C_\infty}\left(\vec{d}\cdot\vec{n}\right), \quad \text{(force optimization)} \end{aligned} \tag{28}$$

the complete variation of the cost functions for the inverse design and force optimization are

$$\begin{aligned} \delta\left(\frac{1}{2}\int_S \left(\Delta C_p\right)^2 ds\right) &= \int_S \left(\frac{\Delta C_p}{C_\infty}(\delta\vec{x}\cdot\vec{\nabla}P) + \mathrm{K}\frac{\left(\Delta C_p\right)^2}{2}\right) ds - I_{eq} \\ \delta\int_S C_p\left(\vec{n}\cdot\vec{d}\right) ds &= \int_S \left(\frac{1}{C_\infty}(\vec{n}\cdot\vec{d})(\delta\vec{x}\cdot\vec{\nabla}P) + \mathrm{K}C_p(\vec{d}\cdot\vec{n}) + C_p(\vec{d}\cdot\delta\vec{n})\right) ds - I_{eq} \\ \text{where } I_{eq} &= \int_S (\vec{n}\cdot\delta\vec{v})\left(\rho\psi_1 + \rho\vec{v}\cdot\vec{\varphi} + \rho H\psi_4\right) ds, \quad \vec{n}\cdot\delta\vec{v}\big|_S = -\left[\left(\delta\vec{x}\cdot\vec{\nabla}\right)\vec{v}\right]\cdot\vec{n} - \delta\vec{n}\cdot\vec{v} \end{aligned} \tag{29}$$

Notice that even though I_{eq} in Eq. (29) contains the variation of the velocity vector $\delta\vec{v}$, it is not necessary to solve the linearized flow equations (16) to actually compute its value. Indeed, I_{eq} only involves the normal component of $\delta\vec{v}$ on the wall, whose value in terms of geometric quantities and flow field variables is given by the linearized boundary condition (17).

It is interesting to compare the results in Eq. (29) to previous works, such as, for example, Eqs. (27a)–(28b) in[7], and particularly to Eq. (27) for the variation of the inverse design cost function in Jameson-Kim's reduced gradient formulation[15], which, although presented in a seemingly different form, is exactly the same as in Eq. (29).

Finally, plugging in Eq. (29) the actual values of K, $\delta\vec{x}$, $\delta\vec{n}$ from Eqs. (11)–(13) and integrating by parts where appropriate, using $\partial_{tg}\vec{t} = \kappa\vec{n}$, $\partial_{tg}\vec{n} = -\kappa\vec{t}$ and $\int_S \left(\partial_{tg} f(s)\right) ds = 0$, Eq. (29) can be cast in the form

$$\begin{aligned} \delta\left(\frac{1}{2}\int_S \left(\Delta C_p\right)^2 ds\right) &= \int_S \left(\frac{\Delta C_p}{C_\infty}\partial_n P - \kappa\frac{\left(\Delta C_p\right)^2}{2}\right)\alpha ds - I_{eq}, \\ \delta\int_S C_p\left(\vec{n}\cdot\vec{d}\right) ds &= \int_S \frac{1}{C_\infty}(\vec{d}\cdot\vec{\nabla}P)\alpha ds - I_{eq} \\ \text{where } I_{eq} &= -\int_S \left((\vec{\nabla}\cdot\vec{v})\left(\rho\psi_1 + \rho\vec{v}\cdot\vec{\varphi} + \rho H\psi_4\right) + (\vec{t}\cdot\vec{v})\partial_{tg}\left(\rho\psi_1 + \rho\vec{v}\cdot\vec{\varphi} + \rho H\psi_4\right)\right)\alpha ds \end{aligned} \tag{30}$$

where $\partial_n = \vec{n}\cdot\vec{\nabla}$ is the normal derivative to the surface S. As is clear from Eq. (30), the final expressions for the complete variations do not depend on the tangent component β of the deformation, as expected. Likewise, the (normal) deformation parameter has been isolated so that the variation can be written in the generic form

$$\delta J = \int_S G\alpha ds \tag{31}$$

where, for example, the expression for force optimization problems is

$$G = \frac{1}{C_\infty}(\vec{d}\cdot\vec{\nabla}P) + (\vec{\nabla}\cdot\vec{v})\left(\rho\psi_1 + \rho\vec{v}\cdot\vec{\varphi} + \rho H\psi_4\right) + (\vec{t}\cdot\vec{v})\partial_{tg}\left(\rho\psi_1 + \rho\vec{v}\cdot\vec{\varphi} + \rho H\psi_4\right) \tag{32}$$

Notice that G is essentially a local gradient. As such, it gives for each point on the surface the optimal deformation direction, that is to say, the size of the deformation in the normal direction which produces the largest variation in the cost function. This result opens the possibility to substitute the standard deformation functions (such as Hicks-Henne functions, Bézier polynomials, etc.) by G (with the appropriate modifications to account for possible geometric restrictions).

Repeating the calculus for a more general pressure-dependent cost function such as $\int_S g(P,\vec{n})ds$, the variation is

$$\delta\int_S g(P,\vec{n})ds = \int_S\left(\frac{\partial g}{\partial P}(\delta\vec{x}\cdot\vec{\nabla}P) + \frac{\partial g}{\partial\vec{n}}\cdot\delta\vec{n} + \mathrm{K}g(P,\vec{n})\right)ds - I_{eq} \tag{33}$$

where I_{eq} is the same as in Eq. (29), and the following boundary conditions hold

$$\begin{aligned}
&\vec{n}\cdot\vec{v}\big|_S = 0\\
&\vec{n}\cdot\delta\vec{v}\big|_S = -\left[\left(\delta\vec{x}\cdot\vec{\nabla}\right)\vec{v}\right]\cdot\vec{n} - \delta\vec{n}\cdot\vec{v}\\
&\vec{n}\cdot\vec{\varphi}\big|_S = \frac{\partial g}{\partial P}
\end{aligned} \tag{34}$$

Proceeding with Eq. (33) as in the derivation of Eq. (30), the following expression is obtained

$$\delta\int_S g(P,\vec{n})ds = \int_S\left[\frac{\partial g}{\partial P}\partial_n P + \left(\partial_{tg}\frac{\partial g}{\partial\vec{n}}\right)\cdot\vec{t} - \kappa\left(g - \frac{\partial g}{\partial\vec{n}}\cdot\vec{n}\right)\right]\alpha ds - I_{eq} \tag{35}$$

which gives

$$\begin{aligned}
G = {} & \frac{\partial g}{\partial P}\partial_n P + \left(\partial_{tg}\frac{\partial g}{\partial\vec{n}}\right)\cdot\vec{t} - \kappa\left(g - \frac{\partial g}{\partial\vec{n}}\cdot\vec{n}\right) + (\vec{\nabla}\cdot\vec{v})\left(\rho\psi_1 + \rho\vec{v}\cdot\vec{\varphi} + \rho H\psi_4\right) + \\
& (\vec{t}\cdot\vec{v})\partial_{tg}\left(\rho\psi_1 + \rho\vec{v}\cdot\vec{\varphi} + \rho H\psi_4\right)
\end{aligned} \tag{36}$$

in the general case.

To sum up this epigraph, the conventional continuous approach does not admit cost functions other than those already presented and combinations thereof (such as aerodynamic efficiency, defined as the ratio between the lift and drag coefficients C_L/C_D). As a matter of fact, cost functions which do not depend exclusively on the pressure do not lead a priori to well posed adjoint sytems[7-9]. However, on closer inspection it can be shown[10] that it is possible to lift such restriction if the flow equations restricted to the boundary are explicitly taken into account. In this way it would be possible to treat non-conventional or incomplete cost functionals[10], as opposed to complete functions which in the inviscid case depend solely on the pressure and do not require explicit insertion of the flow equations on the boundary, but this strategy will not be pursued in this work.

C. Aerodynamic design with the Navier-Stokes equations

The governing equations, for viscous laminar flows in two dimensions, are

$$\vec{\nabla}\cdot\vec{F} = \vec{\nabla}\cdot\vec{F}^{\mathrm{v}} \quad \text{in } \Omega \tag{37}$$

where $\vec{F} = (F_x, F_y)$ has been defined in Eq. (5) and

$$F_x^{\mathrm{v}} = \begin{pmatrix} 0 \\ \sigma_{xx} \\ \sigma_{xy} \\ u\sigma_{xx} + v\sigma_{xy} + k\dfrac{\partial T}{\partial x} \end{pmatrix}, \quad F_y^{\mathrm{v}} = \begin{pmatrix} 0 \\ \sigma_{xy} \\ \sigma_{yy} \\ u\sigma_{yx} + v\sigma_{yy} + k\dfrac{\partial T}{\partial y} \end{pmatrix} \tag{38}$$

The viscous stresses may be written as

$$\sigma_{xx} = \frac{2}{3}\mu\left(2\frac{\partial u}{\partial x} - \frac{\partial v}{\partial y}\right), \quad \sigma_{xy} = \sigma_{yx} = \mu\left(\frac{\partial u}{\partial y} + \frac{\partial v}{\partial x}\right), \quad \sigma_{yy} = \frac{2}{3}\mu\left(2\frac{\partial v}{\partial y} - \frac{\partial u}{\partial x}\right) \tag{39}$$

where μ is the laminar viscosity coefficient. The coefficient of thermal conductivity and the temperature are computed as

$$k = \frac{c_p}{\mathrm{Pr}}\mu, \quad T = \frac{P}{R\rho} \tag{40}$$

where c_p is the specific heat at constant pressure, *Pr* is the Prandtl number and *R* is the gas constant. Turbulent flows can be incorporated by adding to μ the turbulent viscosity coefficient μ_t, whose value is computed by means of a suitable turbulence model, but this possibility will not be considered in this work[‡‡]. Equations (37) are supplemented with characteristic-type boundary conditions on the far field, and non-slip conditions on solid walls

$$u = v = 0 \text{ on } S. \tag{41}$$

An additional boundary condition has to be imposed on the temperature on solid walls, which can be either adiabatic or isothermal (constant temperature)

$$\begin{aligned} \partial_n T\big|_S = \vec{n}\cdot\vec{\nabla}T\big|_S = 0 \qquad & \text{adiabatic,} \\ T\big|_S = T_0 \qquad & \text{constant temperature.} \end{aligned} \tag{42}$$

The corresponding linearized flow equations are, from Eqs. (37) to (42) –see[8]–

$$\begin{aligned} &\vec{\nabla}\cdot\left(\left(\vec{A} + \vec{A}^{v}\right)^{T} M^{-1}\delta U\right) - \partial_x\left(D_{xx}{}^{T} M^{-1}\frac{\partial}{\partial x}\delta U + D_{xy}{}^{T} M^{-1}\frac{\partial}{\partial y}\delta U\right) - \\ &\partial_y\left(D_{yx}{}^{T} M^{-1}\frac{\partial}{\partial x}\delta U + D_{yy}{}^{T} M^{-1}\frac{\partial}{\partial y}\delta U\right) = 0 \quad \text{in } \Omega \end{aligned} \tag{43}$$

‡‡ The generalization of the continuous adjoint approach to include the Spalart-Allmaras turbulence model is currently under investigation and will be the object of a separate publication.

where the matrices are

$$\vec{A} = \left(\frac{\partial \vec{F}}{\partial V}\right)^T, \quad \vec{A}^v = -\left(\frac{\partial \vec{F}^v}{\partial V}\right)^T$$
$$D_{xx} = \left(\frac{\partial F^v{}_x}{\partial(\partial_x V)}\right)^T, \quad D_{xy} = \left(\frac{\partial F^v{}_x}{\partial(\partial_y V)}\right)^T, \quad D_{yx} = \left(\frac{\partial F^v{}_y}{\partial(\partial_x V)}\right)^T, \quad D_{yy} = \left(\frac{\partial F^v{}_y}{\partial(\partial_y V)}\right)^T \tag{44}$$

supplemented with the following boundary conditions

$$\begin{aligned}
&L^{-1}\delta U\Big|_{\text{incoming characteristics}} = 0 \quad \text{on } \Gamma_\infty \\
&\delta u\big|_S = -\delta\vec{x}\cdot\vec{\nabla}u = -\alpha\partial_n u \\
&\delta v\big|_S = -\delta\vec{x}\cdot\vec{\nabla}v = -\alpha\partial_n v \\
&\vec{n}\cdot\vec{\nabla}\delta T\Big|_S = -\delta\vec{n}\cdot\vec{\nabla}T - n_i\delta x_j\partial_j\partial_i T \qquad \text{Adiabatic} \\
&\delta T\big|_S = -\delta\vec{x}\cdot\vec{\nabla}T \qquad \text{Constant temperature}
\end{aligned} \tag{45}$$

where summation over repeated indices is understood, i.e.

$$n_i\delta x_j\partial_j\partial_i T = n_x\delta x_x\partial_x\partial_x T + n_x\delta x_y\partial_y\partial_x T + n_y\delta x_x\partial_x\partial_y T + n_y\delta x_y\partial_y\partial_y T. \tag{46}$$

The issue of defining relevant cost functions and determining their variations is considered next. The structure of the complete objective functions can be determined by examining the boundary terms which arise when the adjoint equation is derived from the linearized flow equations in the way discussed in the previous section. Incomplete objective functions are also possible at the cost of explicitly introducing the restriction of the flow equations to the boundary, but such approach will not be followed here.

As was done in the inviscid case, the linearized flow equations are multiplied by the vector of adjoint variables and integrated over the domain Ω. The resulting expression is then integrated by parts to produce a domain term, and boundary terms supported on the solid wall and far field boundaries. Vanishing of the domain term is tantamount to the adjoint flow equations

$$\begin{aligned}
&\left(M^{-1}\right)^T\left(\vec{A}+\vec{A}^v\right)\cdot\vec{\nabla}\Psi^T + \frac{\partial}{\partial x}\left(\left(M^{-1}\right)^T\left[D_{xx}\frac{\partial\Psi^T}{\partial x} + D_{yx}\frac{\partial\Psi^T}{\partial y}\right]\right) + \\
&\frac{\partial}{\partial y}\left(\left(M^{-1}\right)^T\left[D_{xy}\frac{\partial\Psi^T}{\partial x} + D_{yy}\frac{\partial\Psi^T}{\partial y}\right]\right) = 0.
\end{aligned} \tag{47}$$

The terms supported on the far field boundary can be eliminated with appropriate boundary conditions for the adjoint variables. Finally, the contribution at the solid wall boundary yields the following relation

$$\begin{aligned}
&\int_S\left(\vec{n}\cdot\delta\vec{v}\left(\rho\psi_1 + \rho H\psi_4\right) - \psi_4\vec{n}\cdot\sigma\cdot\delta\vec{v} + \vec{n}\cdot\Sigma\cdot\delta\vec{v}\right)ds + \\
&\int_S\left(k\left(\partial_n\psi_4\right)\delta T - \psi_4\left(\delta k\right)\partial_n T - k\psi_4\partial_n\delta T\right)ds + \int_S\left(\vec{n}\cdot\vec{\varphi}\delta P - \vec{n}\cdot\delta\sigma\cdot\vec{\varphi}\right)ds = 0
\end{aligned} \tag{48}$$

where non-slip boundary conditions have been already enforced on the velocity components, and

$$\vec{n}\cdot\Sigma\cdot\delta\vec{v} = n_x\Sigma_{xx}\delta u + n_x\Sigma_{xy}\delta v + n_y\Sigma_{yx}\delta u + n_y\Sigma_{yy}\delta v$$
$$\Sigma_{xx} = \frac{2}{3}\mu\left(2\frac{\partial\psi_2}{\partial x} - \frac{\partial\psi_3}{\partial y}\right), \quad \Sigma_{xy} = \Sigma_{yx} = \mu\left(\frac{\partial\psi_2}{\partial y} + \frac{\partial\psi_3}{\partial x}\right), \quad \Sigma_{yy} = \frac{2}{3}\mu\left(2\frac{\partial\psi_3}{\partial y} - \frac{\partial\psi_2}{\partial x}\right) \tag{49}$$
$$\delta k = \frac{c_p}{\mathrm{Pr}}\delta\mu$$

In view of Eqs. (45) and (48), the following combination of cost functions and adjoint boundary conditions are possible on adiabatic walls

$$\int_S g\left(\vec{f},T\right)ds, \quad \vec{f} = P\vec{n} - \vec{n}\cdot\sigma$$
$$\left(\psi_2,\psi_3\right) = \left(\frac{\partial g}{\partial f_x},\frac{\partial g}{\partial f_y}\right), \quad k\partial_n\psi_4 = \frac{\partial g}{\partial T} \tag{50}$$

with the corresponding variation being

$$\delta\int_S g\left(\vec{f},T\right)ds = \int_{\delta S} g ds - I_{eq}$$
$$\text{where } I_{eq} = \int_S \left((\vec{n}\cdot\delta\vec{v})\left(\rho\psi_1 + \rho H\psi_4\right) - \psi_4\vec{n}\cdot\sigma\cdot\delta\vec{v} + \vec{n}\cdot\Sigma\cdot\delta\vec{v} - k\psi_4\partial_n\delta T\right)ds \tag{51}$$
$$\delta\vec{v} = -\alpha\partial_n\vec{v}, \quad \partial_n\delta T = -\delta\vec{n}\cdot\vec{\nabla}T - n_i\delta x_j\partial_j\partial_i T$$

and on constant temperature walls

$$\int_S h\left(\vec{f},k\partial_n T\right)ds, \quad \vec{f} = P\vec{n} - \vec{n}\cdot\sigma$$
$$\left(\psi_2,\psi_3\right) = \left(\frac{\partial h}{\partial f_x},\frac{\partial h}{\partial f_y}\right), \quad \psi_4 = -\frac{\partial h}{\partial(k\partial_n T)} \tag{52}$$

with variation

$$\delta\int_S h\left(\vec{f},k\partial_n T\right)ds = \int_{\delta S} h ds - I_{eq}$$
$$\text{where } I_{eq} = \int_S \left((\vec{n}\cdot\delta\vec{v})\left(\rho\psi_1 + \rho H\psi_4\right) - \psi_4\vec{n}\cdot\sigma\cdot\delta\vec{v} + \vec{n}\cdot\Sigma\cdot\delta\vec{v} + k\left(\partial_n\psi_4\right)\delta T\right)ds \tag{53}$$
$$\delta\vec{v} = -\alpha\partial_n\vec{v}, \quad \delta T = -\delta\vec{x}\cdot\vec{\nabla}T$$

Therefore, the Navier-Stokes equations allow a priori optimization with respect to any of the components of the total force exerted by the fluid on the wall (including both the pressure and the viscous stress terms), as well as with respect to surface temperature distributions –for adiabatic boundary conditions– or surface heat flux –for constant temperature boundary conditions –see[8]. It should be noticed, however, that from the above expressions it is clear that functions that depend solely on the pressure are allowed. This is a possibility that has been largely ignored in the literature, so it is worthwhile to discuss it in some detail.

The result follows from noticing that functions such as those in either Eq. (50) or Eq. (52) with the following structure

$$\int_S g\left(\vec{f}\cdot\vec{n}\right)ds \tag{54}$$

–were the possible dependence on the temperature has been ignored– actually depend on the pressure alone, since

$$\vec{f}\cdot\vec{n}\Big|_S = P - \vec{n}\cdot\sigma\cdot\vec{n}\Big|_S = P \tag{55}$$

where, for steady flows

$$(\vec{n}\cdot\sigma\cdot\vec{n})\Big|_S = 0 \tag{56}$$

For such objective functions the shape variation is as follows

$$\delta\int_S g(P)\,ds = \int_S\left(\frac{dg}{dP}(\delta\vec{x}\cdot\vec{\nabla}P) + \mathrm{K}g(P)\right)ds + \int_S\left(\frac{dg}{dP}\delta P\right)ds \tag{57}$$

The last term can be computed from Eq. (48) as

$$\int_S\left(\frac{dg}{dP}\delta P\right)ds = \int_S\frac{dg}{dP}\left(\vec{n}\cdot\delta\sigma\cdot\vec{n}\right)ds - I_{eq} \tag{58}$$

provided that the adjoint variables satisfy the following boundary conditions

$$\vec{\varphi}\Big|_S = \frac{dg}{dP}\vec{n} \tag{59}$$

The a priori unknown term in Eq. (58) containing the variation of the stress tensor can be obtained from the linearization of relation (56)

$$\vec{n}\cdot\delta\sigma\cdot\vec{n}\Big|_S + 2\delta\vec{n}\cdot\sigma\cdot\vec{n}\Big|_S + n_i n_j\delta\vec{x}\cdot\vec{\nabla}\sigma_{ij} = 0 \tag{60}$$

from where it finally follows

$$\delta\int_S g(P)\,ds = \int_S\left(\frac{dg}{dP}(\delta\vec{x}\cdot\vec{\nabla}P) + \mathrm{K}g(P)\right)ds - \int_S\frac{dg}{dP}\left(2\delta\vec{n}\cdot\sigma\cdot\vec{n} + n_i n_j\delta\vec{x}\cdot\vec{\nabla}\sigma_{ij}\right)ds - I_{eq} \tag{61}$$

The result of Eq. (61) can be illustrated by the case of prescribed surface pressure. For such case the cost function is customarily defined as[7, 9]

$$J = \frac{1}{2}\int_S\left(\widetilde{\Delta C_p}\right)^2 ds, \qquad \widetilde{\Delta C_p} = \Delta C_p - \frac{1}{C_\infty}(\vec{n}\cdot\sigma\cdot\vec{n}), \tag{62}$$

which is actually $J = \frac{1}{2}\int_S \left(\Delta C_p\right)^2 ds$ once Eq. (56) is taken into account. According to Eq. (61), this function has a variation

$$\delta J = \int_S \left(\frac{\Delta C_p}{C_\infty} \delta \vec{x} \cdot \left(\vec{\nabla} P - n_j n_i \vec{\nabla} \sigma_{ij} \right) + \frac{1}{2} \mathrm{K} \left(\Delta C_p \right)^2 - 2 \frac{\Delta C_p}{C_\infty} (\delta \vec{n} \cdot \sigma \cdot \vec{n}) \right) ds - I_{eq} \tag{63}$$

and requires the following adjoint boundary conditions

$$\begin{aligned} \left(\psi_2, \psi_3\right)\big|_S &= \frac{\Delta C_p}{C_\infty} \left(n_x, n_y\right) \\ \partial_n \psi_4 \big|_S &= 0, \quad \text{(Adiabatic)} \\ \psi_4 \big|_S &= 0, \quad \text{(Constant temperature)} \end{aligned} \tag{64}$$

To end this section, the cost functions for force optimization problems will be spelled out in detail. The function for total (i.e. including viscous effects) force optimization is

$$\begin{aligned} J &= \int_S \left(\vec{f}^* \cdot \vec{d} \right) ds \\ \vec{f}^* = C_p \vec{n} - \frac{1}{C_\infty} \vec{n} \cdot \sigma, \quad \vec{d} &= \begin{cases} \left(\cos\alpha, \sin\alpha\right) & \text{(Drag)} \\ \left(-\sin\alpha, \cos\alpha\right) & \text{(Lift)} \end{cases} \end{aligned} \tag{65}$$

which has a variation

$$\delta J = \int_S \left(\frac{1}{C_\infty} \left((\delta \vec{x} \cdot \vec{\nabla} P)(\vec{n} \cdot \vec{d}) - n_i d_j \delta \vec{x} \cdot \vec{\nabla} \sigma_{ij} \right) + \mathrm{K} \left(\vec{f}^* \cdot \vec{d} \right) + \delta \vec{n} \cdot \left(C_p \vec{d} - \frac{1}{C_\infty} \sigma \cdot \vec{d} \right) \right) ds - I_{eq} \tag{66}$$

and requires the adjoint boundary conditions

$$\begin{aligned} \left(\psi_2, \psi_3\right)\big|_S &= \frac{1}{C_\infty} \left(d_x, d_y\right) \\ \partial_n \psi_4 \big|_S &= 0, \quad \text{(adiabatic)} \\ \psi_4 \big|_S &= 0, \quad \text{(constant temperature)} \end{aligned} \tag{67}$$

From the above discussion it is clear that it is also possible to consider optimization problems involving the pressure force alone. The resulting formulae follow from Eqs. (59) and (61).

As can be seen from the above results, sensitivity derivatives for viscous flows generically require the computation of second order derivatives of the flow variables –see for example Eqs. (51), which involves the Hessian of the temperature through the linearization of the adiabatic boundary condition, and (66), which involves the gradient of the stress tensor. This has been known for some time[7] and has been in fact pinpointed as the major drawback of the continuous adjoint formulation on unstructured grids, as the accurate numerical evaluation of such derivatives requires at least third-order accuracy, which is beyond the capabilities of most unstructured flow solvers.

It will be shown in the next section that it is possible to reduce the order of derivatives by using the restriction of the (steady state) flow equations to the boundary

$$\begin{aligned}
&\vec{\nabla}\cdot\vec{v}=0\\
&\vec{\nabla}\cdot\sigma=\vec{\nabla}P\\
&\vec{\nabla}\cdot\left(k\vec{\nabla}T\right)=-\sigma:\nabla v\\
&\text{where } \sigma:\nabla v \doteq \sigma_{ij}\partial_i v_j=\sigma_{xx}\partial_x u+\sigma_{xy}\partial_x v+\sigma_{yx}\partial_y u+\sigma_{yy}\partial_y v
\end{aligned} \tag{68}$$

III. Reduction of the higher derivative terms

The first term to be considered, which involves second derivatives of the temperature, appears in I_{eq} on solid walls with adiabatic boundary conditions –see Eq. (51)– and thus affects the computation of every cost function on such walls. It has the form

$$I_{eq}=\ldots-\int_S k\psi_4\left(\partial_n\delta T\right)ds=\ldots+\int_S k\psi_4 n_i\delta x_j\left(\partial_j\partial_i T\right)ds \tag{69}$$

The Hessian operator $\partial_i\partial_j$ on S can be expressed in terms of tangent and normal derivatives. Tangent derivatives pose no problem as they can be readily integrated by parts, thereby reducing the number of derivatives. Normal derivatives, on the other hand, cannot be integrated by parts along S, but can be converted into tangent derivatives by using the flow equations and boundary conditions on S. The idea is as follows. Taking into account Eq. (12), Eq. (69) can be recast in the form

$$\begin{aligned}
&\int_S k\psi_4 n_i\delta x_j\left(\partial_i\partial_j T\right)ds=\int_S k\psi_4\alpha n_i n_j\left(\partial_i\partial_j T\right)ds+\int_S k\psi_4\beta n_i t_j\left(\partial_i\partial_j T\right)ds=\\
&\int_S \alpha k\psi_4\left(\partial_n{}^2 T\right)ds+\int_S k\psi_4\beta\left(\partial_{tg}\partial_n T\right)ds+\int_S k\psi_4\beta\kappa\left(\partial_{tg}T\right)ds=\\
&\int_S \alpha k\psi_4\left(\partial_n{}^2 T\right)ds-\cancel{\int_S \partial_{tg}\left(k\psi_4\beta\right)\left(\partial_n T\right)ds}+\int_S k\psi_4\beta\kappa\left(\partial_{tg}T\right)ds
\end{aligned} \tag{70}$$

where the following identities have been used

$$\begin{aligned}
&\partial_{tg}\doteq\vec{t}\cdot\vec{\nabla}=t_i\partial_i,\quad \partial_n\doteq\vec{n}\cdot\vec{\nabla}=n_i\partial_i\\
&n_i n_j\partial_i\partial_j=\partial_n{}^2,\quad t_i t_j\partial_i\partial_j=\partial_{tg}{}^2-\kappa\partial_n\\
&n_i t_j\partial_i\partial_j=\partial_n\partial_{tg}=\partial_{tg}\partial_n+\kappa\partial_{tg}
\end{aligned} \tag{71}$$

As for the term containing two normal derivatives, it can be rewritten as follows

$$k\partial_n{}^2 T\big|_S=\vec{\nabla}\left(k\vec{\nabla}T\right)\Big|_S-\partial_{tg}\left(k\partial_{tg}T\right)=-\sigma:\nabla v-\partial_{tg}\left(k\partial_{tg}T\right) \tag{72}$$

where use has been made of the energy equation on the boundary –see Eq. (68)– as well as of the Neumann boundary condition for the temperature. Introducing Eq. (72) into Eq. (70) the following expression results

$$\int_S k\psi_4 n_i\delta x_j\left(\partial_i\partial_j T\right)ds=-\int_S\alpha\psi_4\left(\sigma:\nabla v\right)ds-\int_S\alpha\psi_4\partial_{tg}\left(k\partial_{tg}T\right)ds+\int_S k\psi_4\beta\kappa\left(\partial_{tg}T\right)ds. \tag{73}$$

There still remains a term with two tangent derivatives, which can be tackled by integration by parts

$$\int_S k\psi_4 n_i \delta x_j \left(\partial_i \partial_j T\right) ds = -\int_S \alpha\psi_4 \left(\sigma : \nabla v\right) ds + \int_S k\partial_{tg}\left(\alpha\psi_4\right)\left(\partial_{tg} T\right) ds + \int_S k\psi_4 \beta\kappa \left(\partial_{tg} T\right) ds. \tag{74}$$

Hence, the final expression results for I_{eq} on adiabatic solid walls

$$\begin{aligned} I_{eq} &= \int_S (\vec{n}\cdot\delta\vec{v})\left(\rho\psi_1 + \rho H\psi_4\right) ds + \int_S \left(\vec{n}\cdot\Sigma\cdot\delta\vec{v}\right) ds - \int_S \psi_4 \left(\vec{n}\cdot\sigma\cdot\delta\vec{v}\right) ds \\ &+ \int_S k\psi_4 \left(\delta\vec{n}\cdot\vec{\nabla}T\right) ds - \int_S \alpha\psi_4 \left(\sigma : \nabla v\right) ds + \int_S k\partial_{tg}\left(\alpha\psi_4\right)\left(\partial_{tg} T\right) ds + \int_S k\psi_4 \beta\kappa \left(\partial_{tg} T\right) ds. \end{aligned} \tag{75}$$

Equation (75) can be further reduced by noting that, from Eq. (13),

$$\delta\vec{n} = -\left(\beta\kappa + \partial_{tg}\alpha\right)\vec{t} \tag{76}$$

which, when substituted into Eq. (75) yields

$$\begin{aligned} I_{eq} &= \int_S (\vec{n}\cdot\delta\vec{v})\left(\rho\psi_1 + \rho H\psi_4\right) ds + \int_S \left(\vec{n}\cdot\Sigma\cdot\delta\vec{v}\right) ds \\ &- \int_S \psi_4 \left(\vec{n}\cdot\sigma\cdot\delta\vec{v}\right) ds - \int_S \alpha\psi_4 \left(\sigma : \nabla v\right) ds + \int_S k\alpha \left(\partial_{tg}\psi_4\right)\left(\partial_{tg} T\right) ds. \end{aligned} \tag{77}$$

Taking into account that $\delta\vec{v} = -\alpha\partial_n\vec{v}$, Eq. (77) can be written as

$$I_{eq} = \int_S \left(-(\vec{n}\cdot\partial_n\vec{v})\left(\rho\psi_1 + \rho H\psi_4\right) - \vec{n}\cdot\Sigma\cdot\partial_n\vec{v} + \psi_4\left(\vec{n}\cdot\sigma\cdot\partial_n\vec{v}\right) - \psi_4\left(\sigma : \nabla v\right) + k\left(\partial_{tg}\psi_4\right)\left(\partial_{tg} T\right)\right)\alpha ds \tag{78}$$

Additional terms containing second derivatives of the velocity field appear for cost functions involving the stress tensor –see Eqs. (63) and (66). For force optimization problems the disturbing term is of the form

$$\begin{aligned} &-\int_S n_i d_j \left(\delta\vec{x}\cdot\vec{\nabla}(\sigma_{ij})\right) ds = -\int_S n_i d_j \delta x_k \partial_k(\sigma_{ij}) ds = \\ &-\int_S \alpha d_j n_i n_k \left(\partial_k \sigma_{ij}\right) ds - \int_S \beta d_j n_i t_k \left(\partial_k \sigma_{ij}\right) ds = -\int_S \alpha d_j n_i \left(\partial_n \sigma_{ij}\right) ds - \int_S \beta d_j n_i \left(\partial_{tg}\sigma_{ij}\right) ds. \end{aligned} \tag{79}$$

As before, the trick is to convert the normal derivatives to tangent derivatives by resorting to the flow equations. It follows from the identity

$$n_i \partial_n \sigma_{ij} \equiv \vec{n}\cdot\partial_n\sigma = \vec{\nabla}\cdot\sigma - \vec{t}\cdot\partial_{tg}\sigma \tag{80}$$

and the momentum equation, $\vec{\nabla}\cdot\sigma\big|_S = \vec{\nabla}P$, that Eq. (79) can be cast in the form

$$\begin{aligned} &-\int_S n_i d_j (\delta\vec{x}\cdot\vec{\nabla}(\sigma_{ij})) ds = -\int_S \alpha d_j \left(\partial_i \sigma_{ij}\right) ds + \int_S \alpha t_i d_j \left(\partial_{tg}\sigma_{ij}\right) ds - \int_S \beta n_i d_j \left(\partial_{tg}\sigma_{ij}\right) ds = \\ &-\int_S \alpha\left(\vec{d}\cdot\vec{\nabla}P\right) ds - \int_S \delta x_i^{\perp} d_j \left(\partial_{tg}\sigma_{ij}\right) ds = -\int_S \left(\delta\vec{x}\cdot\vec{n}\right)\left(\vec{d}\cdot\vec{\nabla}P\right) ds + \int_S \vec{d}\cdot\sigma\cdot\left(\partial_{tg}\delta\vec{x}^{\perp}\right) ds \end{aligned} \tag{81}$$

where

$$\delta\vec{x}^{\perp} = \beta\vec{n} - \alpha\vec{t} \tag{82}$$

Therefore, from Eqs. (66) and (81) it follows that

$$\begin{aligned}
&\delta\int_S \left(C_p(\vec{n}\cdot\vec{d}) - \frac{1}{C_\infty}(\vec{n}\cdot\sigma\cdot\vec{d}) \right) ds = \frac{1}{C_\infty}\int_S \left((\delta\vec{x}\cdot\vec{\nabla}P)(\vec{n}\cdot\vec{d}) - n_i d_j \delta\vec{x}\cdot\vec{\nabla}\sigma_{ij} \right) ds \\
&+\int_S \left(\mathrm{K}\left(C_p(\vec{n}\cdot\vec{d}) - \frac{1}{C_\infty}(\vec{n}\cdot\sigma\cdot\vec{d}) \right) + \delta\vec{n}\cdot\left(C_p\vec{d} - \frac{1}{C_\infty}\sigma\cdot\vec{d} \right) \right) ds - I_{eq} = \\
&\frac{1}{C_\infty}\int_S \left((\delta\vec{x}\cdot\vec{\nabla}P)(\vec{n}\cdot\vec{d}) - (\delta\vec{x}\cdot\vec{n})\left(\vec{d}\cdot\vec{\nabla}P\right) \right) ds + \int_S \left(C_p\vec{d}\cdot(\delta\vec{n} + \mathrm{K}\vec{n}) \right) ds \\
&+\frac{1}{C_\infty}\int_S \left(\vec{d}\cdot\sigma\cdot\left(\partial_{tg}\delta\vec{x}^{\perp} - \mathrm{K}\vec{n} - \delta\vec{n} \right) \right) ds - I_{eq}
\end{aligned} \tag{83}$$

where like terms have been grouped for later convenience. It is possible to further reduce Eq. (83) by using Eqs. (11) –(13) and (82), which can be combined in the identity

$$\mathrm{K}\vec{n} + \delta\vec{n} = \left(\partial_{tg}\beta - \alpha\kappa \right)\vec{n} - \left(\beta\kappa + \partial_{tg}\alpha \right)\vec{t} = \partial_{tg}\delta\vec{x}^{\perp} \tag{84}$$

Likewise,

$$\frac{1}{C_\infty}\left((\delta\vec{x}\cdot\vec{\nabla}P)(\vec{n}\cdot\vec{d}) - (\delta\vec{x}\cdot\vec{n})\left(\vec{d}\cdot\vec{\nabla}P\right) \right) = \frac{1}{C_\infty}\left(\vec{d}\cdot\delta\vec{x}^{\perp} \right)\partial_{tg}P = \left(\vec{d}\cdot\delta\vec{x}^{\perp} \right)\partial_{tg}C_p \tag{85}$$

Together, Eqs. (83), (84) and (85) yield finally

$$\begin{aligned}
&\delta\int_S \left(C_p(\vec{n}\cdot\vec{d}) - \frac{1}{C_\infty}(\vec{n}\cdot\sigma\cdot\vec{d}) \right) ds = \\
&\int_S \left(\left(\partial_{tg}C_p \right)(\vec{d}\cdot\delta\vec{x}^{\perp}) \right) ds + \int_S \left(C_p\vec{d}\cdot(\partial_{tg}\delta\vec{x}^{\perp}) \right) ds - I_{eq} = \int_S \partial_{tg}\left(C_p\vec{d}\cdot\delta\vec{x}^{\perp} \right) ds - I_{eq} = -I_{eq}
\end{aligned} \tag{86}$$

This result leaves for the local gradient G in this case the final expression –see Eq. (78):

$$\begin{aligned}
&\delta\int_S \left(C_p(\vec{n}\cdot\vec{d}) - \frac{1}{C_\infty}(\vec{n}\cdot\sigma\cdot\vec{d}) \right) ds = \int_S G\alpha ds \\
&G = (\vec{n}\cdot\partial_n\vec{v})\left(\rho\psi_1 + \rho H\psi_4 \right) + \vec{n}\cdot\Sigma\cdot\partial_n\vec{v} - \psi_4\left(\vec{n}\cdot\sigma\cdot\partial_n\vec{v} \right) + \psi_4\left(\sigma : \nabla v \right) - k\left(\partial_{tg}\psi_4 \right)\left(\partial_{tg}T \right)
\end{aligned} \tag{87}$$

As for inverse design problems, the reduction of the higher derivative terms makes it possible to rewrite the expression (63) as

$$\delta\frac{1}{2}\int_S \left(\Delta C_p \right)^2 ds = \int_S \left[-\frac{1}{2}\alpha\kappa\left(\Delta C_p \right)^2 + \frac{\Delta C_p}{C_\infty}\left(\vec{t}\cdot\sigma\cdot\vec{n} \right)\partial_{tg}\alpha - \frac{\alpha}{C_\infty}\left(\vec{t}\cdot\sigma\cdot\vec{n} \right)\partial_{tg}\Delta C_p \right] ds - I_{eq} \tag{88}$$

IV. Extension to 3D

The previous results can be readily extended to the case of 3D flows. The governing equations are a direct generalization of (37)

$$\frac{\partial F^i}{\partial x^i} = \frac{\partial F^{vi}}{\partial x^i} \quad \text{in } \Omega \tag{89}$$

with

$$U = \begin{pmatrix} \rho \\ \rho u^1 \\ \rho u^2 \\ \rho u^3 \\ \rho E \end{pmatrix}, \qquad F^i = \begin{pmatrix} \rho u^i \\ \rho u^i u^1 + P\delta_{i1} \\ \rho u^i u^2 + P\delta_{i2} \\ \rho u^i u^3 + P\delta_{i3} \\ \rho u^i H \end{pmatrix}, \qquad F^{vi} = \begin{pmatrix} 0 \\ \sigma_{ij}\delta_{j1} \\ \sigma_{ij}\delta_{j2} \\ \sigma_{ij}\delta_{j3} \\ u^j\sigma_{ij} + k\dfrac{\partial T}{\partial x^i} \end{pmatrix} \tag{90}$$

where u^1, u^2, u^3 are the Cartesian velocity components, δ_{ij} is the Kronecker delta function, and

$$\sigma_{ij} = \mu\left(\frac{\partial u^i}{\partial x^j} + \frac{\partial u^j}{\partial x^i} - \frac{2}{3}\delta_{ij}\frac{\partial u^k}{\partial x^k}\right) \tag{91}$$

are the viscous stresses. In what follows, latin indices from the middle of the alphabet $i, j, k, \ldots = 1,2,3$ will denote 3D Cartesian coordinates, $x^i = (x, y, z)$. Repeated index "*i*" implies summation over *i* = 1 to 3.

The solid walls will be represented in 3D by a closed surface *S* (or union thereof) described by a parametrization $\vec{x}(\xi,\eta) = (x(\xi,\eta), y(\xi,\eta), z(\xi,\eta))$ with parameters (ξ,η) which we shall refer collectively to as ξ^a, with latin indices from the beginning of the alphabet $a, b, c, \ldots = 1,2$ denoting parametric directions on the surface. Let $\vec{e}_a$ denote the tangent vectors to the surface corresponding to the given (ξ,η) parametrization, and assume that the parametrization is picked such that $\vec{N} = (\vec{e}_1 \times \vec{e}_2)/|\vec{e}_1 \times \vec{e}_2|$ is the exterior unit normal to the surface. The integration measure is now $dS = |\vec{e}_1 \times \vec{e}_2| d\xi d\eta$. A generic deformation of the boundary can be described as follows

$$\delta\vec{x}(\xi,\eta) = \alpha(\xi,\eta)\vec{N} + \beta^a(\xi,\eta)\vec{e}_a \tag{92}$$

For sufficiently small values of the deformation, the following holds

$$\begin{aligned} \delta\vec{e}_a &= \left(\partial_a\alpha + \beta^b L_{ab}\right)\vec{N} + \left(\partial_a\beta^b + \beta^c\Gamma^b_{ca} - \alpha L_{ac}g^{cb}\right)\vec{e}_b \\ \delta\vec{N} &= -g^{ab}\left(\partial_a\alpha + \beta^c L_{ac}\right)\vec{e}_b \\ \delta dS &= \left(\partial_a\beta^a + \beta^c\Gamma^a_{ca} - \alpha L_{ab}g^{ab}\right)dS = \left(\vec{\nabla}_{tg}\cdot\vec{\beta} - 2\mathrm{H}_m\alpha\right)dS \end{aligned} \tag{93}$$

where g^{ab} is the inverse metric tensor, L_{ab} is the second fundamental form, Γ^c_{ab} are the Christoffel symbols and $\mathrm{H}_m = L_{ab}g^{ab}/2$ is the mean curvature of the surface –hence, in passing from 2D to 3D the replacement $\mathrm{K}_{2D} = \partial_{tg}\beta - \kappa\alpha \to \mathrm{K}_{3D} = \vec{\nabla}_{tg}\cdot\vec{\beta} - 2\mathrm{H}_m\alpha$ needs to be done in the curvature term of the geometric part of the variation (3).

As in 2D, the analysis of the variation of the usual objective functions (lift/drag, inverse design) unveils terms containing the second derivative of the flow variables. Proceeding as above, these terms can be reduced, resulting in

$$\delta\int_S\left(C_p(\vec{N}\cdot\vec{d})-\frac{1}{C_\infty}(\vec{N}\cdot\sigma\cdot\vec{d})\right)dS=-I_{eq}=\int_S G\alpha dS$$
$$G=(\vec{N}\cdot\partial_n\vec{u})\left(\rho\psi_1+\rho H\psi_5\right)+\vec{N}\cdot\Sigma\cdot\partial_n\vec{u}-\psi_5\left(\vec{N}\cdot\sigma\cdot\partial_n\vec{u}\right)+\psi_5\left(\sigma_{ij}\partial_i u_j\right)-k\left(\vec{\nabla}_{tg}\psi_5\right)\cdot\left(\vec{\nabla}_{tg}T\right) \tag{94}$$

for lift/drag optimization problems. Also, for prescribed surface pressure the following expression results:

$$\delta\frac{1}{2}\int_S\left(\Delta C_p\right)^2 ds=\int_S\left[-\alpha\mathrm{H}_m\left(\Delta C_p\right)^2+\frac{\Delta C_p}{C_\infty}\left(\vec{N}\cdot\sigma\cdot\vec{\nabla}_{tg}\alpha\right)-\frac{\alpha}{C_\infty}\left(\vec{N}\cdot\sigma\cdot\vec{\nabla}_{tg}\Delta C_p\right)\right]ds-I_{eq} \tag{95}$$

V. Brief description of the numerical implementation and summary of results

All the final formulas of this paper have been implemented in the 2D finite-volume code NENS (developed by INTA) that solves the Navier-Stokes equations on unstructured meshes using an edge based structure. In order to simplify the adjoint implementation, most of the original direct solver subroutines have been used (edge structure, time integration, multigrid scheme, etc).

The analytical expressions developed in this paper have been tested and some results are shown to demonstrate the quality of the gradients calculated using this approach in Euler and laminar Navier-Stokes problems. Also, a full optimization problem is exhibited with the purpose of demonstrating the potentiality of the developed software.

A. Numerical implementation

1. Spatial discretization

A finite volume discretization is used to solve the direct and adjoint equations. The finite volume discretization is obtained by applying the integral formulation of the governing equations to the control volume surrounding a node. A time marching strategy is used to obtain the steady solution[16, 17]. For the adjoint equation

$$\frac{\partial}{\partial t}\int_{c_i}\Psi d\Omega-\int_{\partial c_i}\overline{F}\vec{n}dl+\left[\int_{\partial c_i}\overrightarrow{F^v}\vec{n}dl+\int_{c_i}Q^v d\Omega\right]=0\rightarrow\frac{\partial}{\partial t}\left(\Psi_i\Omega_i\right)=\sum_{k=1}^{neighbour}f_{ik}S_{ik}-\left[\sum_{k=1}^{neighbour}f_{ik}^vS_{ik}+Q_i^vV_i\right] \tag{96}$$

Where Ψ is the vector of adjoint variables, $\overline{F}$ is the adjoint convective flux, $\overrightarrow{F^v}$ is the adjoint viscous flux, Q^v is an adjoint viscous source term, the surfaces S_{ik} enclose the control volume for the node i (dual mesh). The schemes for the adjoint convective flux are based on a central discretization with dissipation terms of either artificial dissipation type or upwind flux. The artificial dissipation between two nodes *0* and *1* could be expressed as follows

$$d_{01}=\varepsilon\left(\nabla^2\Psi_0-\nabla^2\Psi_1\right)\varphi_{01}\lambda_{01}$$
where
$$\nabla^2\Psi_0=\sum_{k=1}^{neighbour}\left(\Psi_k-\Psi_0\right)=-n_0\Psi_0+\sum_{k=1}^{neighbour}\left(\Psi_k\right) \tag{97}$$
$$\lambda_{01}=\left(\left|\vec{u}_{01}\cdot\vec{n}_{01}\right|+c_{01}\right)S_{01},\ \vec{u}_{01}=\frac{\vec{u}_0+\vec{u}_1}{2},\ c_{01}=\frac{c_0+c_1}{2}$$

Where ε is a calibrated parameter, λ_{01} is the local spectral radius, ∇^2 denotes the undivided Laplacian operator, $\vec{u}_{01}$ and c_{01} denote the fluid speed and sound speed at the cell face, $\vec{n}_{01}$ denotes the normal direction of the control surface to the edge between nodes *0*, *1* and S_{01} its size.

If an upwind scheme is used, the system of adjoint equations can be expressed (in one dimension) as

$$\frac{\partial \Psi}{\partial t} - \frac{\partial F}{\partial x} = 0 \rightarrow \frac{\partial \Psi}{\partial t} - \frac{\partial F}{\partial \Psi}\frac{\partial \Psi}{\partial x} = \frac{\partial \Psi}{\partial t} - A^T \frac{\partial \Psi}{\partial x} = 0 \tag{98}$$

Where A^T is the transpose of the Jacobian inviscid matrix flux. Using a 1D finite volume method, the discretization around the node *i* has the following form

$$\begin{aligned} \Psi_i^{n+1} &= \Psi_i^n - \frac{\Delta t}{\Delta x}\left[F_{i+1/2}^n(\Psi) - F_{i-1/2}^n(\Psi)\right] \\ F_{i+1/2} &= F_i^+ + F_{i+1}^- = 1/2\,A^T\left(\Psi_{i+1} - \Psi_i\right) - 1/2\left|A^T\right|\left(\Psi_{i+1} - \Psi_i\right) \\ F_{i-1/2} &= F_{i-1}^+ + F_i^- = 1/2\,A^T\left(\Psi_i - \Psi_{i-1}\right) - 1/2\left|A^T\right|\left(\Psi_i - \Psi_{i-1}\right) \end{aligned} \tag{99}$$

2. Steady state time integration

In order to speed up the rate of convergence an overset multigrid scheme is used and the Jacobian matrices are linear interpolated between the different mesh levels. The iterative algorithm employed is an explicit q-stage Runge-Kutta scheme.

3. Boundary conditions

The boundary conditions for the solid-wall are imposed in two ways: using a ghost cell scheme adapted to unstructured meshes or directly imposing the boundary conditions on the analytical flux expressions. On the far field a characteristics method is used.

B. Design variables

Concerning the design variables, different possibilities have been tested: deformation or bump functions such as Wagner polynomials, Hicks-Vanderplaats functions, Legendre polynomials, Hicks-Henne functions, Bézier polynomials, NURBS; modifications in the thickness and camber line and also individual surface node movement.

In this article, the shape functions introduced by Hicks-Henne[18] have been used.

$$\Delta y = \sum_{k=1}^{N} \delta_k f_k(x), f_k(x) = \sin^3\left(\pi x^{e_k}\right) \quad \text{with} \quad e_k = \frac{\log(0.5)}{\log(x_k)} \tag{100}$$

Where N is the number of bump functions and δ_k is the design variable step. Each shape function has its maximum at the point x_k and these functions are separately applied to the upper and lower surface.

C. Mesh deformation

A matricial method is used to move 2D meshes. The matricial method is based in the definition of a stiffness matrix that connects the two ends of a single bar (mesh edge). All the quantities must be stored using a sparse method and a conjugate gradient algorithm is used to solve the linear system.

$$\begin{bmatrix} F_{X_i} \\ F_{Y_i} \\ M_{\theta_i} \\ F_{X_j} \\ F_{Y_j} \\ M_{\theta_j} \end{bmatrix} = [R]^T \cdot [k_L] \cdot [R] \cdot \begin{bmatrix} X_i \\ Y_i \\ \theta_i \\ X_j \\ Y_j \\ \theta_j \end{bmatrix} \tag{101}$$

where the matrix $[R]$ is the rotational matrix, F and M are forces and torques, respectively. Finally the stiffness matrix has this form

$$[k_L] = \begin{bmatrix} \frac{AE}{L} & 0 & 0 & \frac{-AE}{L} & 0 & 0 \\ 0 & \frac{12EI}{L^3} & \frac{6EI}{L^2} & 0 & \frac{-12EI}{L^3} & \frac{6EI}{L^2} \\ 0 & \frac{6EI}{L^2} & \frac{4EI}{L} & 0 & \frac{-6EI}{L^2} & \frac{2EI}{L} \\ \frac{-AE}{L} & 0 & 0 & \frac{AE}{L} & 0 & 0 \\ 0 & \frac{-12EI}{L^3} & \frac{-6EI}{L^2} & 0 & \frac{12EI}{L^3} & \frac{-6EI}{L^2} \\ 0 & \frac{6EI}{L^2} & \frac{2EI}{L} & 0 & \frac{-6EI}{L^2} & \frac{4EI}{L} \end{bmatrix} \tag{102}$$

where L is the bar length and the values of the A (bar area), E (elasticity modulus) and I (moment of inertia) are up to the designer.

D. The optimization framework

The continuous adjoint formulation allows the computation of a wide range of different objective functions: quadratic deviation from a target pressure (inverse design), drag minimization, lift maximization, pitching moment, aerodynamic efficiency, and linear combinations. Also, several constrains have been implemented: non-dimensional flow parameters (minimum lift, maximum drag, etc.) and geometrical estimations (maximum and minimum thickness, curvature, volume, area, etc.).

The modularity must be a fundamental characteristic in optimal design software: The program *ACTIV*[19] is used to compute the objective function values and gradients using control theory; and the program *Optimizer* is used to find an optimum using gradient and non-gradient based strategies. In this case, gradient based optimization, the program *Optimizer* uses an INTA's version of the program *CONMIN*[20] that is a well-known program for the solution of non-linear constrained optimization problems. The *CONMIN* uses feasible search direction obtained from a compromise between gradients of objective functions and imposed constraints. In each design iteration the *CONMIN* program requires as inputs the values and gradients of the objective functions and constraints.

E. Summary of results

In this section some relevant results are shown. The Hicks-Henne bump functions have been used as design variables. The first design variable has its maximum close to the trailing edge on the lower side of the airfoil, and the following variables translate the maximum in the clockwise direction.

The gradients computed with the adjoint method described in this paper are compared with a standard finite-difference method where the finite step of the design variable must be adequately selected depending on the characteristics of the flow. The finite-difference gradients are obtained by forward differencing.

1. Euler transonic redesign of a NACA 0012 airfoil

A single-point optimization case is used to show the accuracy of the developed continuous adjoint method for inviscid flows. The flow conditions are Mach number 0.8 with angle of attack 1.25 degrees. The governing equations are the Euler equations, so drag improvement in this case mean wave drag decrease.

In Fig. 1 a comparison between the drag gradients computed by finite-difference and the adjoint method is shown. The agreement is very good, with some minor discrepancies, likely owing to the finite step in finite-difference computations, becoming visible in the upper side of the airfoil downstream of the shock wave.

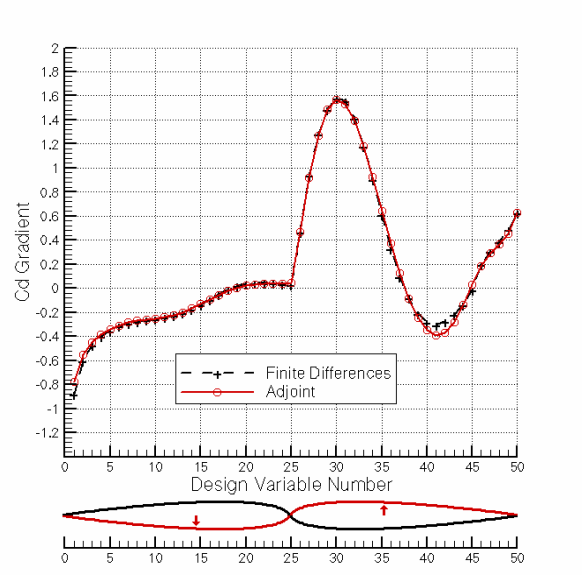

Figure 1. Inviscid Cd transonic gradients

In the proposed transonic design problem, the objective function is the minimization of the wave drag, increasing the lift to 0.34 and with a minimum thickness of 10%, keeping the angle of attack fixed. The results are shown in Fig. 2, the shock wave has almost disappeared in few iterations.

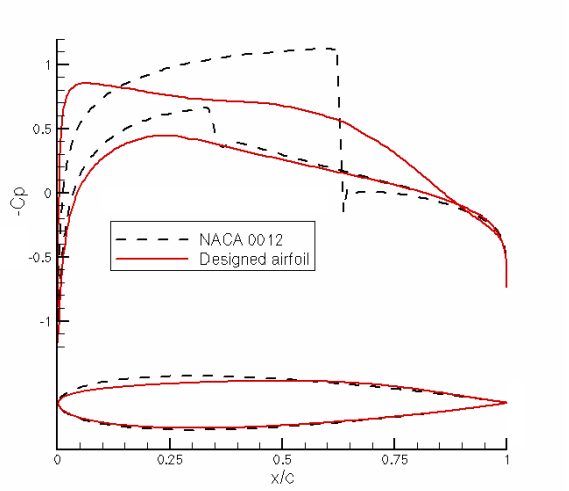

Figure 2. Initial and designed Cp and geometry

After the optimization process the new airfoil has a drag coefficient of 0.0012, which is a 5% of the original NACA 0012 drag (overall reduction of 200 counts). Also, the final lift coefficient is a 105% greater that the original one.

2. Viscous subsonic gradients of a cylinder

The main objective of this example is to evaluate the accuracy of the viscous drag gradients computed by means of the proposed continuous adjoint method for laminar viscous flows in a well-known subsonic problem. We are using a simple configuration of a cylinder faced with a low velocity flow (Mach number 0.1) and a low Reynolds number of 50 that leads to a steady flow solution of the problem.

This test case clearly illustrates the necessity of the reduction of the second order derivative terms. In Fig. 3, the finite-difference gradients are compared with the gradients computed with the adjoint method (with and without the reduction of the second order derivative terms)

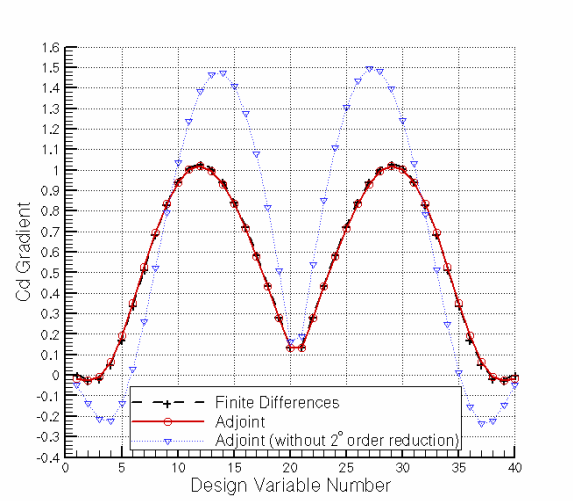

Figure 3. Inviscid Cd subsonic gradients

In conclusion, the continuous adjoint approach provides very accurate gradients in a highly sensitive problem like this. Also, the importance of the reduction of second order derivative terms for obtaining numerical results of quality should be emphasized.

3. Viscous subsonic redesign of a NACA 0012 airfoil

To study the accuracy of the developed methodology, a case of viscous laminar flow is selected. The flow conditions are Mach number equal to 0.3, angle of attack of 2.50º and low Reynolds number of 1000 to keep the laminar flow along the airfoil. The proposed design problem starts with the flow conditions described above, the objective is drag minimization, increasing the lift to 0.15, using 3 geometrical constraints: minimum value for the greatest thickness (12%), frozen curvature at the leading edge and minimum thickness at 75% of the chord.

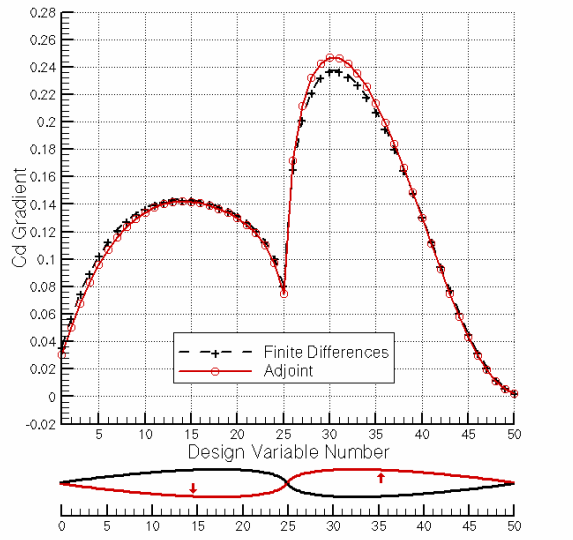

Figure 4. Laminar Navier Stokes Cd subsonic gradients

In Fig. 4 a comparison between the gradients computed by finite-difference and adjoint methods is shown. The agreement is excellent, in order to obtain these results a hybrid mesh is use with 25 points on the viscous layer that has a thickness of 0.031.

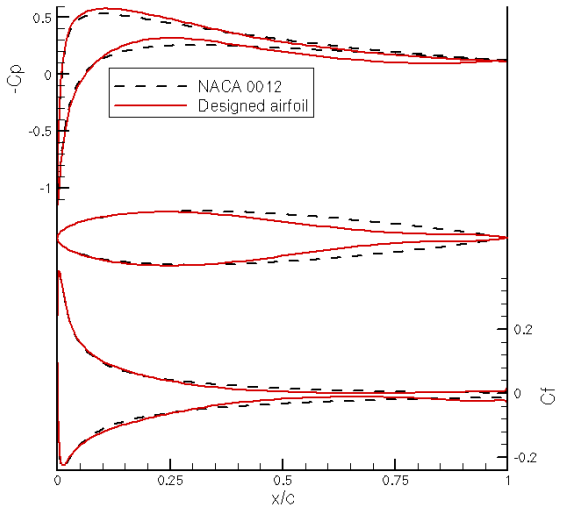

Figure 5. Initial and designed Cp, Cf and geometry

The results of the optimization are shown in Fig. 5. After 9 design cycles the new airfoil based on a NACA 0012 has a drag of 0.1225 that is a 97% of the original NACA 0012 drag (reduction of 36 counts), while the final lift is a 111% greater than the original one.

VI. Conclusions

In this work a systematic continuous adjoint approach to aerodynamic design optimization has been presented. The resulting expressions are suitable for optimization under viscous as well as inviscid flow conditions on unstructured as well as structured grids.

In the past, several drawbacks of the continuous adjoint approach for viscous flows on unstructured grids have been pointed out. One of the upshots of this work has been the resolution of some of those issues. For example, the need for accurate second order derivatives of the flow variables required for computing sensitivity derivatives for viscous flows has been solved with the development of a systematic way of reducing the order of the higher derivative terms. Also, the class of admissible optimization functionals has been clarified and, in particular, it has been shown that for viscous flows, and contrary to what seems to have been taken for certain so far, arbitrary functions of the pressure *alone* can be naturally optimized.

The accuracy of the sensitivity derivatives that result from the application of the method developed in this work has been assessed by comparison with finite-difference computations, and the validity of the overall methodology has been illustrated with several design examples.

The results presented here are promising, but further work is necessary. Additional numerical tests are necessary. Also, work to extend the methodology to deal with general turbulent three-dimensional flows (including the continuous adjoint formulation of the Spalart-Allmaras turbulence model) is currently in progress. We expect to report on these and related issues in the near future. Finally, a hybrid continuous-discrete adjoint scheme looks like the best solution for adjoint strategies in a future, combining the continuous scheme showed in this article with a discrete adjoint scheme for the space discretization method employed in the direct solution of Navier-Stokes equations.

Appendix

Next, the definition of the Euler and Navier-Stokes Jacobian matrices is presented. The matrices are written in terms of primitive variables $V=(\rho,u,v,P)^T$. Switching to conservative variables $U=(\rho,\rho u,\rho v,\rho E)^T$ is accomplished with the aid of the transformation matrices

$$M=\frac{\partial U}{\partial V}=\begin{pmatrix}1 & \cdot & \cdot & \cdot\\ u & \rho & \cdot & \cdot\\ v & \cdot & \rho & \cdot\\ \frac{\vec{v}^2}{2} & \rho u & \rho u & \frac{1}{(\gamma-1)}\end{pmatrix},\quad M^{-1}=\begin{pmatrix}1 & \cdot & \cdot & \cdot\\ -\frac{u}{\rho} & \frac{1}{\rho} & \cdot & \cdot\\ -\frac{v}{\rho} & \cdot & \frac{1}{\rho} & \cdot\\ \frac{(\gamma-1)\vec{v}^2}{2} & (1-\gamma)u & (1-\gamma)v & (\gamma-1)\end{pmatrix}. \tag{103}$$

The Euler Jacobian matrices take the form

$$A_x=\left(\frac{\partial F_x}{\partial V}\right)^T=\begin{pmatrix}u & u^2 & uv & \frac{1}{2}u\vec{v}^2\\ \rho & 2\rho u & \rho v & \rho\left(H+u^2\right)\\ \cdot & \cdot & \rho u & \rho uv\\ \cdot & 1 & \cdot & \frac{u\gamma}{(\gamma-1)}\end{pmatrix},\quad A_y=\left(\frac{\partial F_y}{\partial V}\right)^T=\begin{pmatrix}v & uv & v^2 & \frac{1}{2}v\vec{v}^2\\ \cdot & \rho v & \cdot & \rho uv\\ \rho & \rho u & 2\rho v & \rho\left(H+v^2\right)\\ \cdot & \cdot & 1 & \frac{v\gamma}{(\gamma-1)}\end{pmatrix}, \tag{104}$$

whereas, for the viscous flux the appropriate matrices are

$$A^v{}_x=-\left(\frac{\partial F^v{}_x}{\partial V}\right)^T=\begin{pmatrix}\cdot & -\frac{\partial\mu}{\partial\rho}\hat{\sigma}_{xx} & -\frac{\partial\mu}{\partial\rho}\hat{\sigma}_{xy} & -\frac{\partial\mu}{\partial\rho}\left(\hat{\sigma}_{xx}u+\hat{\sigma}_{xy}v+\frac{\gamma}{(\gamma-1)\mathrm{Pr}}\frac{\partial}{\partial x}\left(\frac{P}{\rho}\right)\right)+\frac{\gamma}{(\gamma-1)\mathrm{Pr}}\mu\frac{\partial}{\partial x}\left(\frac{P}{\rho^2}\right)\\ \cdot & \cdot & \cdot & -\sigma_{xx}\\ \cdot & \cdot & \cdot & -\sigma_{xy}\\ \cdot & -\frac{\partial\mu}{\partial P}\hat{\sigma}_{xx} & -\frac{\partial\mu}{\partial P}\hat{\sigma}_{xy} & -\frac{\partial\mu}{\partial P}\left(\hat{\sigma}_{xx}u+\hat{\sigma}_{xy}v+\frac{\gamma}{(\gamma-1)\mathrm{Pr}}\frac{\partial}{\partial x}\left(\frac{P}{\rho}\right)\right)-\frac{\gamma}{(\gamma-1)\mathrm{Pr}}\mu\frac{\partial}{\partial x}\left(\frac{1}{\rho}\right)\end{pmatrix}$$

$$A^v{}_y=-\left(\frac{\partial F^v{}_y}{\partial V}\right)^T=\begin{pmatrix}\cdot & -\frac{\partial\mu}{\partial\rho}\hat{\sigma}_{yx} & -\frac{\partial\mu}{\partial\rho}\hat{\sigma}_{yy} & -\frac{\partial\mu}{\partial\rho}\left(\hat{\sigma}_{yx}u+\hat{\sigma}_{yy}v+\frac{\gamma}{(\gamma-1)\mathrm{Pr}}\frac{\partial}{\partial y}\left(\frac{P}{\rho}\right)\right)+\frac{\gamma}{(\gamma-1)\mathrm{Pr}}\mu\frac{\partial}{\partial y}\left(\frac{P}{\rho^2}\right)\\ \cdot & \cdot & \cdot & -\sigma_{yx}\\ \cdot & \cdot & \cdot & -\sigma_{yy}\\ \cdot & -\frac{\partial\mu}{\partial P}\hat{\sigma}_{yx} & -\frac{\partial\mu}{\partial P}\hat{\sigma}_{yy} & -\frac{\partial\mu}{\partial P}\left(\hat{\sigma}_{yx}u+\hat{\sigma}_{yy}v+\frac{\gamma}{(\gamma-1)\mathrm{Pr}}\frac{\partial}{\partial y}\left(\frac{P}{\rho}\right)\right)-\frac{\gamma}{(\gamma-1)\mathrm{Pr}}\mu\frac{\partial}{\partial y}\left(\frac{1}{\rho}\right)\end{pmatrix} \tag{105}$$

where $\hat{\sigma}_{ij}=\partial_i v_j+\partial_j v_i-\frac{2}{3}\delta_{ij}\vec{\nabla}\cdot\vec{v}$, and

$$D_{xx}=\left(\frac{\partial F^{v}_{\ x}}{\partial(\partial_x V)}\right)^T=\begin{pmatrix}\cdot & \cdot & \cdot & -\dfrac{\gamma\mu}{(\gamma-1)\,\mathrm{Pr}}\dfrac{P}{\rho^2}\\ \cdot & \dfrac{4}{3}\mu & \cdot & \dfrac{4}{3}u\mu\\ \cdot & \cdot & \mu & v\mu\\ \cdot & \cdot & \cdot & \dfrac{\gamma}{(\gamma-1)\,\mathrm{Pr}}\dfrac{\mu}{\rho}\end{pmatrix},\quad D_{yx}=\left(\frac{\partial F^{v}_{\ y}}{\partial(\partial_x V)}\right)^T=\begin{pmatrix}\cdot & \cdot & \cdot & \cdot\\ \cdot & \cdot & -\dfrac{2}{3}\mu & -\dfrac{2}{3}v\mu\\ \cdot & \mu & \cdot & u\mu\\ \cdot & \cdot & \cdot & \cdot\end{pmatrix},$$

$$D_{xy}=\left(\frac{\partial F^{v}_{\ x}}{\partial(\partial_y V)}\right)^T=\begin{pmatrix}\cdot & \cdot & \cdot & \cdot\\ \cdot & \cdot & \mu & v\mu\\ \cdot & -\dfrac{2}{3}\mu & \cdot & -\dfrac{2}{3}u\mu\\ \cdot & \cdot & \cdot & \cdot\end{pmatrix},\quad D_{yy}=\left(\frac{\partial F^{v}_{\ y}}{\partial(\partial_y V)}\right)^T=\begin{pmatrix}\cdot & \cdot & \cdot & -\dfrac{\gamma\mu}{(\gamma-1)\,\mathrm{Pr}}\dfrac{P}{\rho^2}\\ \cdot & \mu & \cdot & u\mu\\ \cdot & \cdot & \dfrac{4}{3}\mu & \dfrac{4}{3}\mu\\ \cdot & \cdot & \cdot & \dfrac{\gamma}{(\gamma-1)\,\mathrm{Pr}}\dfrac{\mu}{\rho}\end{pmatrix}. \tag{106}$$

In the derivation of the viscous Jacobians in Eq. (105) the dependence of the laminar viscosity and heat conduction coefficients μ and *k* on the flow has been explicitly taken into account. If boundary deformations result in large variations of those coefficients (that is to say, if δμ and δ*k* are not negligible), then the corresponding terms in Eq. (105) must be taken into account when solving the adjoint equations. Otherwise, these terms can be dropped, which notably simplifies the resulting expressions

$$A^{\mathrm{v}}_{\ x}=-\left(\frac{\partial F^{v}_{\ x}}{\partial V}\right)^T=\begin{pmatrix}\cdot & \cdot & \cdot & \dfrac{\gamma}{(\gamma-1)\,\mathrm{Pr}}\mu\dfrac{\partial}{\partial x}\left(\dfrac{P}{\rho^2}\right)\\ \cdot & \cdot & \cdot & -\sigma_{xx}\\ \cdot & \cdot & \cdot & -\sigma_{xy}\\ \cdot & \cdot & \cdot & -\dfrac{\gamma}{(\gamma-1)\,\mathrm{Pr}}\mu\dfrac{\partial}{\partial x}\left(\dfrac{1}{\rho}\right)\end{pmatrix},\quad A^{\mathrm{v}}_{\ y}=-\left(\frac{\partial F^{v}_{\ y}}{\partial V}\right)^T=\begin{pmatrix}\cdot & \cdot & \cdot & \dfrac{\gamma}{(\gamma-1)\,\mathrm{Pr}}\mu\dfrac{\partial}{\partial y}\left(\dfrac{P}{\rho^2}\right)\\ \cdot & \cdot & \cdot & -\sigma_{yx}\\ \cdot & \cdot & \cdot & -\sigma_{yy}\\ \cdot & \cdot & \cdot & -\dfrac{\gamma}{(\gamma-1)\,\mathrm{Pr}}\mu\dfrac{\partial}{\partial y}\left(\dfrac{1}{\rho}\right)\end{pmatrix} \tag{107}$$

Acknowledgments

The research described in this paper made by INTA's researchers has been supported under the INTA activity *termofluidodinámica* (INTA's code: IGB4400903) and the Spanish Project DOMINO (CIT-370200-2005-10). Also, this work has been partially supported by the grant BFM2002-03345 of the Spanish MEC.

References

[1]Pironneau, O., "On Optimum Design in Fluid Mechanics," J. Fluid Mech., Vol. 64, 1974, pp. 97-110.

[2]Jameson, A., "Aerodynamic Design Via Control Theory," Journal of Scientific Computing, Vol. 3, 1988, pp. 233-260.

[3]Jameson, A., "Optimum Aerodynamic Design Using CFD And Control Theory," AIAA Paper 95-1729, 1995.

[4]Monge, F. and Palacios, F., "Multipoint Airfoil Optimisation Using Control Theory," *Fourth European Congress on Computational Methods in Applied Sciences and Engineering*, Jyväskylä (Findland), 2004.

[5]Zuazua, E., "Propagation, Observation, and Control of Waves Approximated by Finite Difference Methods," SIAM Review, Vol. 47, No. 2, 2005, pp. 197-243.

[6]Nadarajah, S. K. and Jameson, A., "A Comparison of the Continuous and Discrete Adjoint Approach to Automatic Aerodynamic Optimization," AIAA Paper 2000-0667, 2000.

[7]Anderson, W. K. and Venkatakrishnan, V., "Aerodynamic Design Optimization on Unstructured Grids with a Continuous Adjoint Formulation," AIAA Paper 97-0643, 1997.

[8]Giles, M. B. and Pierce, N. A., "Adjoint Equations in CFD: Duality, Boundary Conditions and Solution Behavior," AIAA Paper 97-1850, 1997.
[9]Jameson, A., Pierce, N. A., and Martinelli, L., "Optimum Aerodynamic Design Using the Navier-Stokes Equations," AIAA Paper 97-0101, 1997.
[10]Arian, E. and Salas, M. D., "Admitting the Inadmissible: Adjoint Formulation for Incomplete Cost Functionals in Aerodynamic Optimization," AIAA Journal, Vol. 37, No. 1, 1999, pp. 37-44.
[11]Jameson, A., Sriram, S., and Martinelli, L., "A Continuous Adjoint Method for Unstructured Grids," AIAA Paper 2003-3955, 16th AIAA CFD Conference, Orlando, Florida, 2003.
[12]Jameson, A., Sriram, S., Martinelli, L., and Haimes, B., "Aerodynamic Shape Optimization of Complete Aircraft Configurations using Unstructured Grids," AIAA Paper 2004-533, 42nd AIAA Aerospace Sciences Meeting and Exhibit, Reno, Nevada,5 - 8 January, 2004.
[13]Hadamard, J., *Leçons sur le calcul des variations*, Gauthier-Villars, Paris, 1910.
[14]Jameson, A., Schmidt, W., and Turkel, E., "Numerical Solution of the Euler Equations by Finite Volume Methods Using Runge-Kutta Time-stepping," AIAA Paper 81-1259, 1981.
[15]Jameson, A. and Kim, S., "Reduction of the Adjoint Gradient Formula in the Continuous Limit," AIAA Paper 2003-0040, 41st AIAA Aerospace Sciences Meeting and Exhibit, Reno (Nevada), January 2003.
[16]Eliasson, P., "EDGE, A Navier-Stokes Solver for Unstructured Grids," FOI Scientific Report, FOI-R-0298-SE, 2002.
[17]Hirsch, C., *Numerical computation of internal and external flows*, John Wiley & Sons ltd, 1984.
[18]Hicks, R. M. and Henne, P. A., "Wing Design by Numerical Optimization," AIAA Aircraft systems & technology meeting. Seattle (Washington), Vol. AIAA Paper 77-1247, August 1977.
[19]Monge, F. and Palacios, F., "Inviscid Multipoint Airfoil Optimisation Using Control Theory," *ERCOFTAC Design Optimisation: Methods & Applications. International Conference & Advanced Course Program*, Athens (Greece), 2004.
[20]Vanderplaats, G. N., "CONMIN - a FORTRAN Program for Constrained Function Minimization: User's Manual," NASA Report, TM-X-62282, 1973.